Power output estimation of a RM3 WEC with HF radar measured complex representative sea states

D. Wang, D. Conley. M. Hann, K. Collins, S. Jin and D. Greaves

Abstract—**Wave tank model testing has been widely used to assess the performance of Wave Energy Converters (WEC) in different technology readiness levels (TRL). At early stage the use of simple wave conditions such as regular waves and parametric wave spectrum JONSWAP or Pierson-Moskowitz spectrum is acceptable. However at later stages there is a need to use site specific complex wave conditions representative of potential prototype deployment sites. In previous research, 10 different regrouping methods on HF radar measured wave spectrum were tested to find out the most representative sea states for tank testing. It has been shown that by using the K-means clustering technique, the characteristics of wave conditions can be well preserved [1, 2]. In order to assess the power capture performance of a typical WEC in these representative sea states, the RM3 point absorber has been simulated. By analysing how well the average power output predicted from different representative sea-state selection methods compares with the total power output prediction, it is shown that the non-directional wave spectrum K-means clustering method provides the most representative sea states and, for a point absorber, with a very accurate estimation of the total power output, which is not the case by using a traditional binning method. The importance of using the complex site-specific sea states rather than simplified parametric JONSWAP sea states to obtain the accurate total power estimation has also been shown.**

Keywords— **HF radar, K-means method, wave spectrum, WEC-SIM, PTO.**

Manuscript received 9 September, 2021; revised 21 December 2021; accepted 26 April, 2021; published 10 June, 2022.

This work was supported in part by the MaRINET2 project.

D. Wang, M. Hann, K. Collins, S. Jin and D. Greaves are with School of Engineering, Computing and Mathematics, University of Plymouth, Devon, U.K. PL4 8AA (e-mail: daming.wang@plymouth.ac.uk).

D. Conley is with School of Biological and Marine Science, University of Plymouth, Devon, U.K. PL4 8AA (e-mail: daniel.conley@plymouth.ac.uk).

Digital Object Identifier https://doi.org/10.36688/imej.5.1-10

I. Introduction

WAVE energy converters (WEC) are devices which can capture wave energy and transform it into electricity [3]. Due to global warming and a necessity to achieve zero net greenhouse gas emission by 2050, research in renewable energy has had more and more attention in recent years. Among different types of renewable energy sources, marine renewable energy (MRE) is considered an energy source with great potential. MRE mainly consists of 6 types, which are wave energy, ocean current energy, tidal energy (tidal range and tidal currents energy [4]), OTEC (ocean thermal energy converter), offshore wind energy and osmotic energy (derived from the difference in the salt concentration between different water layers). Among which wave energy has high power density, however, due to the complexity of waves, the utilization of wave energy is still under-developed. According to estimations, the global potential of wave energy is about 26,000 TWh/yr [5].

In the past few decades, hundreds of WECs have been designed, they can mainly be classified into 4 categories based on operating principle: the oscillating water column (OWC), the oscillating body, the overtopping device and other pressure differential device. In order to describe the development stages needed to commercialize a WEC, the technology Readiness Level (TRL) [6] is used. It partitions the development of WECs from concept validation to final commercialization into 5 stages, the first two stages rely on small-scale tank model testing with scale ranging from 1:100 to 1:10 [7] and is key to de-risking higher TRL stages. Tank testing is an important stage for the development of WECs, but can also be expensive, and it is necessary to select a few suitable sea states for tank testing of the model based on limited resources.

Instruments such as floating buoy, Acoustic Doppler Current Profiler (ADCP), X-band radar and HF radar are used to measure sea states at potential deployment sites in the form of hourly or half-hourly directional wave spectra. Due to the large amount of measured data, selecting a certain number of sea states for tank testing can be challenging. Traditionally, a binning method is used to identify the number of occurrences of particular significant wave height and peak or energy period combinations. Sea states described by these properties are then modelled using a parametric wave spectra such as JONSWAP or

Pierson-Moskowitz while wave directionality is reproduced using a directional spreading function (DSF) [8]. However such an approach represents a simplification of the actual site conditions, where spectral shape and directional spreading may differ from these parametric approaches. Apart from that, the bins selected for tank testing are not representative because not every sea state is included in the bins.

In an attempt to improve the representation of local sea condition, Hamilton [9] applied the K-means clustering method on 2456 non-directional wave spectra measured at Port Hedland, Australia in 1992 to obtain a set of representative sea states. In contrast to the traditional Hs-Tp binning method, the representative sea states take account of the measured spectral shape. This method was later extended into 8 regrouping methods and compared by Draycott [1] to identify 20 and 40 representative sea states from 64673 buoy-measured half-hourly directional wave spectra provided by European Marine Energy Centre (EMEC). Wang [2] created two additional methods based on the K-means method by using 3161 HF radar spectra measured in Cornwall, UK and 8402 floating buoy measured hourly directional spectra in Long island, US to obtain representative sea states.

In this paper, wave data from 10 different regrouping methods are tested on a numerical WEC model, to investigate the power output of the device predicted by each of the different methods.

II. K-MEANS CLUSTERING TECHNIQUE

The K-means method is used to divide a total of N members into K groups, making sure that similar members are put in the same group by minimising the sum of squared error (SSE) of all members. The equation for SSE is given in equation (1) [10]

$$\begin{aligned} \mathrm{SSE} &= \sum_{k=1}^{K} \sum_{\forall x_i \in C_k} ||x_i - \mu_k||^2 \\ &= \sum_{k=1}^{K} \sum_{\forall x_i \in C_k} d(x_i, \mu_k)^2 \end{aligned} \tag{1}$$

In which x_i is the data member, C_k is the set of members in cluster k, μ_k is the vector mean of cluster k. d is the Euclidean distance between two p-dimensional instances, $x_i = (x_{i1}, x_{i2}, \dots, x_{ip})$ and $x_j = (x_{j1}, x_{j2}, \dots, x_{jp})$.

$$\begin{aligned} d(x_i, x_j) = (&|x_{i1} - x_{j1}|^2 \\ &+ |x_{i2} - x_{j2}|^2 + \dots + |x_{ip} \\ &- x_{jp}|^2)^{1/2} \end{aligned} \tag{2}$$

μ_k is defined as:

$$\mu_k = \frac{1}{N_k} \sum_{\forall x_i \in C_k} x_i \tag{3}$$

From the definition of SSE, it can be seen that a good clustering method is one that provides the minimum average difference between group members and their cluster mean. The K-means method provides a very efficient way to minimize SSE, the flow chart of K-means

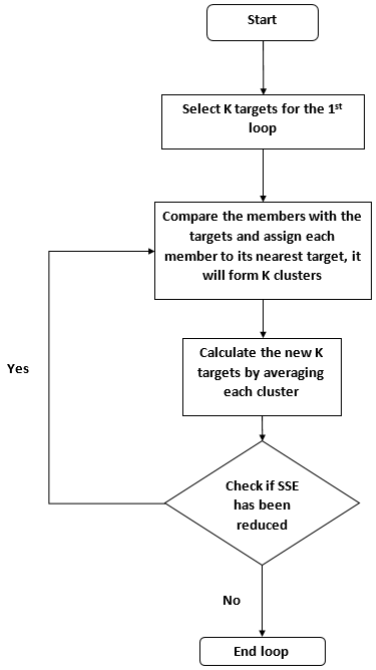

Fig. 1. Flow chart for K-means clustering method.

method is shown in Fig.1. When SSE does not decrease by relocation of the cluster centres, it indicates the current partition is optimal and the iteration can stop.

A disadvantage of K-means clustering method is that the clustering results can be affected by the initial K group centres selected in the first iteration. The commonly used method is to randomly select K initial centres. This can result in different regrouping results when different runs start with different initial group centres. To account for this, the clustering is repeated with multiple initial cluster centres, and the result with the smallest SSE selected.

Here a K-means++ algorithm based on a heuristic scheme with 100 repeats is used to improve the quality of the final solution.

A. *High frequency radar measured sea states.*

The High frequency (HF) radar system is a shore-based remote sensing system which is originally widely used to measure ocean current information. The vertically transmitted polarized electromagnetic waves, which are scattered by the water wave surface, travel back and are received by the HF radar [11]. They are then analysed and two nearly symmetric dominant peaks can be found from the spectra and used to obtain the ocean current velocity [12]. Later on people found that by using two HF radar covering the same ocean area, by processing the back-scattered spectrum with certain inversion algorithms, it is possible obtain the directional wave spectrum ([13], [14]). In this paper, the HF radar data for analysis is obtained by

a two-phased-array Wellen Radars (WERA) system located in the southwest coast of the UK which overlooks a marine renewable testing field (Wave Hub). During 8 months' measurement, there are in total 3161 hourly directional spectra obtained (The HF radar data with low signal to noise ratio are not for use)

Sea states measured by HF radar at Wave Hub from April 2012 to December 2012 are used as the total data set. Each hourly directional wave spectrum is in the units of $m^2/(Hz \cdot rad)$, there are 30 angular directions ranging from 0 rad to $29\pi/15$ rad with an interval of $\pi/15$ rad and 92 frequencies ranging from 0.03Hz to 0.28Hz.

B. *Description of the 10 regrouping methods.*

In previous research by Draycott [1], eight regrouping methods were created and tested on the EMEC buoy measured directional wave spectra. Another two new methods created by Wang [2] are added for the analysis, in total 10 methods are shown in TABLE I.

TABLE I
METHODS USED FOR SEA STATES REGROUPING

Method	Description
A	*Hs,Te binning method*
B	*Hs,Te, θ_m binning method*
C	*S(f) clustering method*
D	*S(f, θ) clustering method*
E	*Hs,Te clustering method*
F	*Hs, Te ,v, θ_m,P, Sp σ_θ clustering method*
G	*Method E+C two-step method*
H	*Method F+D two-step method*
I	*Method C + modified E two-step method*
J	*Method D + modified E two-step method*

Hs is the significant wave height, *Te* is the energy period, θ_m is the mean wave direction, *S(f)* is the non-directional wave spectrum, *S(f,θ)* is the directional wave spectrum, *v* is the spectral bandwidth, *P* is the wave power, *Sp* is the wave steepness, σ_θ is the directional spreading of directional wave.

Method A is a binning method, in which each directional spectrum is transformed and plotted into *Hs-Te* two-dimensional space. By defining the size of the *Hs* and *Te* bins, the total data set can be divided into a number of bins. By averaging each bin members' wave spectrum, the representative sea states can be obtained. This binning method A is different from the traditional H-T binning method, which selects and tests only a few bins from a large number of non-empty bins. A traditional binning method is shown in Fig.2 [15, 16]. From it can be seen not all of the data points are included in the 15 selected bins. Normally those bins are selected subjectively. Usually people tend to select bins with H_s and T_e they are interested in based on different WECs. While for binning method A, each of the non-empty bins must be used.

TABLE II
NUMBER OF BINS FOR METHOD A AND B

Method	No. of Hs bins	No. of Te bins	No. of θ_m bins	No. of non-empty bins
A(K=20)	6	4	-	19
B(K=20)	4	3	3	21

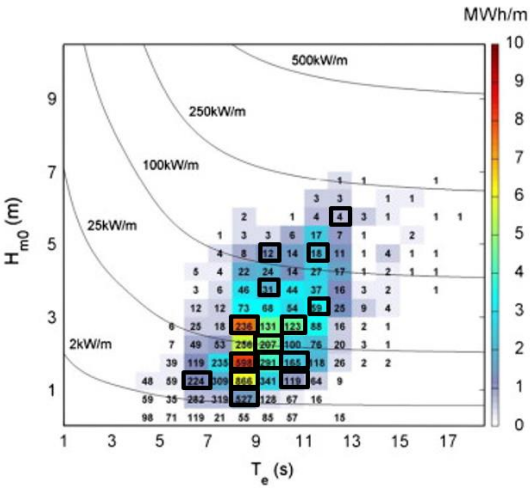

Fig. 2. Traditional binning method of directional annual average scatter diagram of the wave resource at the site considered for a breakwater OWC. All of the 15 bins selected are circled in black for later use in Marinet2 tank testing for an OWC model.

Method B is similar to method A but adding a third dimension θ_m which is the mean wave direction. So the bins are three-dimensional rather than 2-dimensional

Method C is the non-directional wave spectrum K-means clustering method, the difference between two members $S_i(f)$ and $S_j(f)$, $f = (f_1, f_2, \dots, f_p)$ is given in equation (4):

$$d(S_i(f), S_j(f)) = (|S_i(f_1) - S_j(f_1)|^2 + |S_i(f_2) - S_j(f_2)|^2 + \dots + |S_i(f_p) - S_j(f_p)|)^{1/2} \quad (4)$$

For method D, the difference between two members $S_i(f,\theta)$, $S_j(f,\theta)$, $f = (f_1, f_2, \dots, f_p)$, $\theta = (\theta_1, \theta_2, \dots, \theta_q)$ can be calculated by the following equation (5):

$$d\left(S_i(f,\theta), S_j(f,\theta)\right) = \frac{1}{pq}\left[\sum_{m=1}^{p}\sum_{n=1}^{q}(|S_i(f_m,\theta_n) - S_j(f_m,\theta_n)|^2)\right]^{1/2} \quad (5)$$

Method E is K-means method with normalized significant wave height *Hs* and energy period *Te* (Both of the parameters are normalized by their total mean value

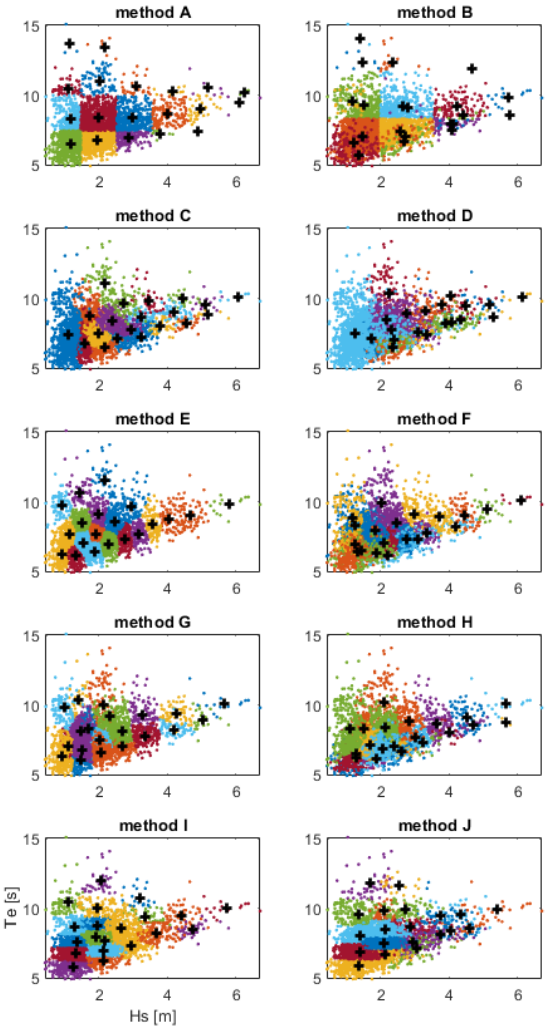

Fig. 3. Regrouping results and their representative sea states (black cross) in *Hs-Te* space for HF radar data when *K*=20. Members in the same group are of the same colour.

respectively). Method F is similar to method E but takes another 5 parameters into consideration which are spectral bandwidth v, wave mean direction θ_m, wave power P, peak steepness S_P and directional spreading parameter σ_θ. All of the parameters are normalized by the mean value of the total data set respectively. Method E and F were also tested by normalizing the parameters by the maximum value of each parameter, however that quality for the regrouping results were negatively affected so in this paper, the parameters used in method E and F are still normalized by their mean value. Method G and H are both two-step methods from which the first step is to create *K*/2 sub-groups by method E or F and the second step is to use C and D to split each sub-cluster into two groups to obtain *K* groups in total. Method I and J are also two-step methods as well but using method C or D as the first step then using a modified method E which balances the importance of normalised *Hs* and *Te* in the clustering process. To show the regrouping results clearly, method A to J and their representative sea states for HF radar data when K=20 are plotted in $H_s - T_e$ space in Fig. 3.

C. *Metric used for assessing different regrouping methods*

In order to compare the quality of different regrouping methods, a metric [17] is used. This metric focuses on the average difference between each group member with its cluster mean. When K clusters are created for a certain method, $k = 1, \dots K$, each group k has a number of members $M(k)$, $m = 1, \dots M(k)$. δ is a certain variable for quality analysis ($\delta = H_s, T_e, \dots S(f), S(f,\theta)$), d represents how many discrete values a certain δ has ($d = 1, \dots D(\delta)$), the metric is defined in equation (6).

$$Met(\delta) = \sum_{k=1}^{K} \frac{1}{K} \sum_{m=1}^{M(k)} \frac{1}{M(k)} \sum_{d=1}^{D(\delta)} \frac{|\delta_{k,m,d} - \mu_{k,d}(\delta)|}{\sum_{d=1}^{D(\delta)} \mu_{k,d}(\delta)} \quad (6)$$

Since this metric represents the average distance of group members from their cluster mean, a lower metric value represents a better regrouping result. From the definition of the metric, its value cannot exceed 1.

In previous research from Draycott [1] and Wang [2], the regrouping quality increases with increasing *K*, which means it is better to use a large K value to identify the representative sea states. However, due to the time constraints of the tank testing, it is not possible to increase K without limit. In this paper, K=20 is used for the analysis.

D. *Quality analysis for different regrouping methods*

After obtaining the sea states for analysis, 10 regrouping methods were tested with HF radar data. For binning method A and B, it is necessary to define the size of bins in order to create *K* non-empty bins. However, it is not an easy task, because the equally sized binning method might create empty bins. After multiple attempts with different

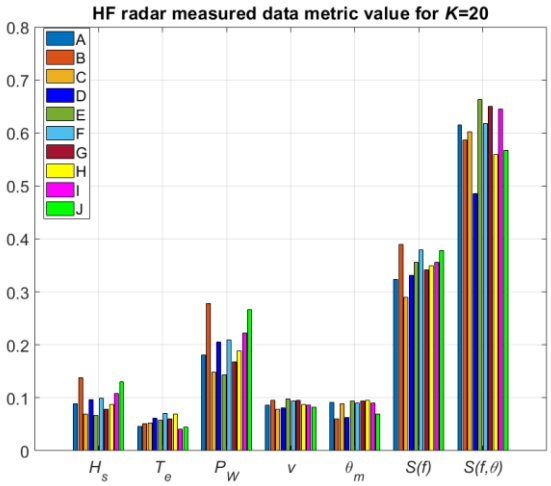

Fig. 4. Metric for HF radar data from method A to J.

H_s and T_e steps, the bins created are shown in TABLE II, It can be seen that the targeted K and the K achieved is still a

little different. All of the non-empty bins are used for the analysis. For other clustering methods C to J, it is easy to obtain 20 groups. The representative sea states is the mean of the directional wave spectra of each group. After obtaining the representative sea states and calculating the metric value for all of the methods. The results of different methods are shown in Fig. 4.

From Fig. 4, it can be seen that the metric for one-dimensional parameters (*Hs, Te, Power, v,* θ_m) is always lower than that of non-directional spectra *S(f)*, the parameter for non-directional spectra is always lower than that of the directional spectra *S(f,θ)*.This is because of the reduction in detail by which individual sea states are defined as they are integrated from *S(f,θ)* to *S(f)*, to one dimensional parameters. [2]

From Fig. 4 it can be seen that method C, which cluster using the individual non-directional wave spectrum, unsurprisingly produces representative sea states with the best 'representation' of the individual non-directional wave spectrum (the lowest metric value for S(f)). Similarly method D, which clusters using the individual directional wave spectrum produces representative sea states that best represent the individual directional wave spectrum (S(f, θ)). For the individual 1D parameters considered method C showed similar or better performance compared to the other methods. The representative sea states generated by Method D performed less well at providing

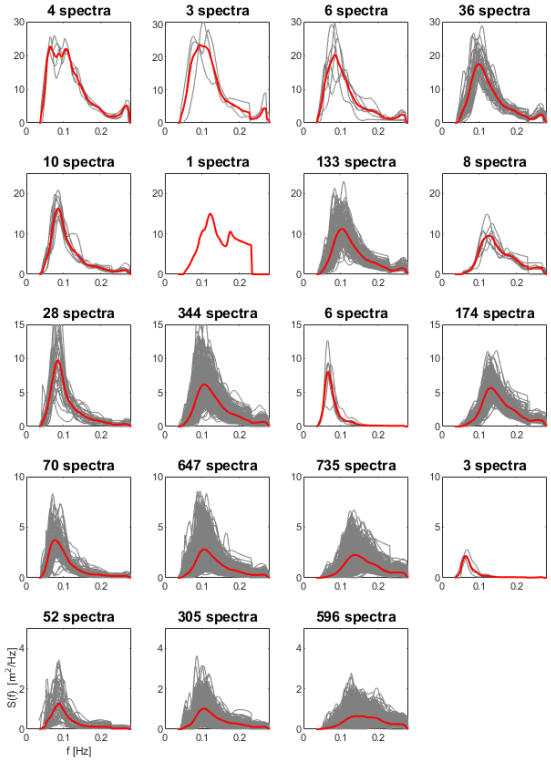

Fig. 5. Each group's wave spectra and their representative sea states in *S(f)* space, title represents the number of each group's members for method A.

a presentation of the sea states power. The binning methods (A and B) performed less well for the majority of parameters.

E. Representative sea states in the form of non-directional wave spectrum.

Taking the regrouping results from method A and method C for comparison, each group's members and their

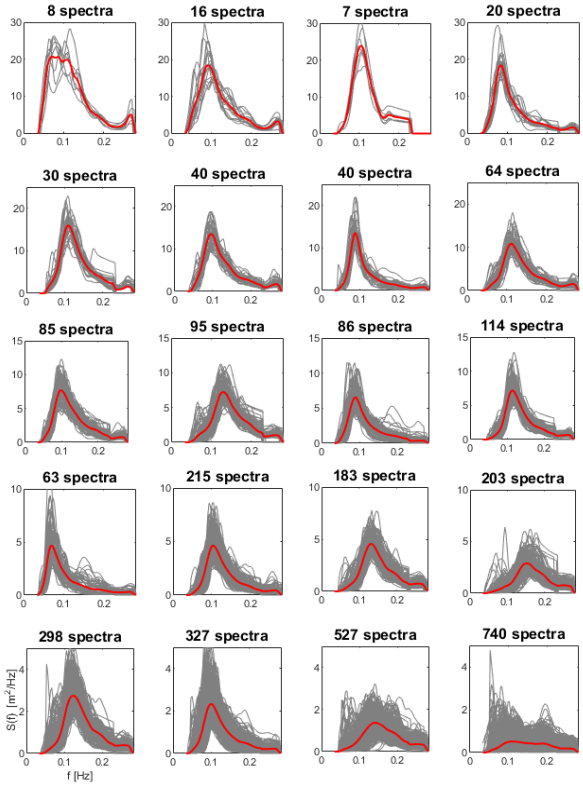

Fig. 6. Each group's wave spectra and their representative sea states in S(f) space, title represents the number of each group's members for method C.

representatives (plotted with red line) are plotted in Fig. 5 and Fig. 6 for comparison. It can be seen that both methods creates 20 (or close to 20 for binning method A) groups; each group has a different number of members inside

III. POWER OUTPUT ESTIMATION WITH NUMERICAL WEC MODEL

F. Representative sea states in the form of non-directional wave spectrum.

After obtaining 20 representative sea states from each method, the next step is to investigate the performance of a WEC using these representative sea states. Here we choose the RM3 point absorber device and use WEC-SIM for the numerical analysis.

The RM3 is established by The U.S. Department of Energy for research and to evaluate the potential for commercial application [18]. It is a two-body point absorber consisting of a float and a spar plate. Geometry dimensions and mass properties of the full-scale prototype are shown in Table III [19] and Fig. 7 [20].

The numerical model of the RM3 point absorber is built with WEC-SIM, an open source WEC analysis tool based on Simulink in MATLAB [19]. WEC-SIM is a time domain analysis software which requires the frequency domain analysis results (hydrodynamic parameters) and the

geometry model of the WEC as input. By defining the sea states and mooring conditions and power take off system (PTO) in WEC-SIM, it can simulate the model in regular waves (sinusoidal waves), non-directional irregular waves and directional irregular waves. The numerical model of RM3 point absorber is provided in WEC-SIM as a tutorial model, due to the simplicity of the model, it is very efficient and each run with 3600s run time only takes 1 min to finish, so the wave energy output analysis for RM3 point absorber is carried out with this numerical model. Non-linear effects are not included in the numerical model.

The numerical model is set up without mooring lines in this study and the incoming wave direction is positive

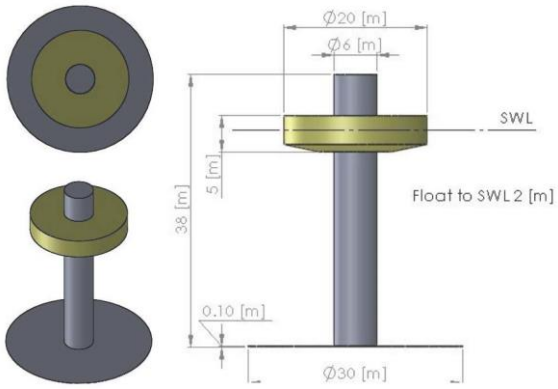

Fig. 7. Geometry dimensions for RM3 point absorber.

TABLE III
DIMENSIONAL PARAMETERS FOR THE WEC

	CoG [m]	Mass [tonne]	Moment of Inertia [kg m^2]		
Float	0	727.01	2.09E+07	0.00E+00	0.00E+00
	0		0.00E+00	2.13E+07	4.30E+03
	-0.72		0.00E+00	4.30E+03	3.71E+07
Spar plate	0	878.3	9.44E+07	0.00E+00	0.00E+00
	0		0.00E+00	9.44E+07	2.18E+05
	-21.29		0.00E+00	2.18E+05	2.85E+07

along the x-axis, i.e. left to right in Fig. 8. Due to the symmetry of the geometry, both of the bodies are restricted to move in 3-DoFs which are surge, heave and pitch. The motion responses are the same for both the float and the spar plate in surge and pitch, and there is relative movement between the two bodies along the spar. There is a translational damping parameter C between the two bodies, the output power is calculated based on the following equation (7):

$$Power = C \cdot |\overrightarrow{v_{re}}| \cdot |\overrightarrow{v_{re}}| \quad (7)$$

In which v_{re} is the relative velocity between the float and the spar plate, C is the translational damping parameter which is 1.2E06 N/m/s.

In order to assess the performance of the model, the representative sea states from the 10 regrouping methods A to J were imported to WEC-SIM for average energy output estimation in the form of non-directional wave spectra. Each non-directional wave spectrum was provided with a frequency dependent random phase angle ranging from 0 to 2π.

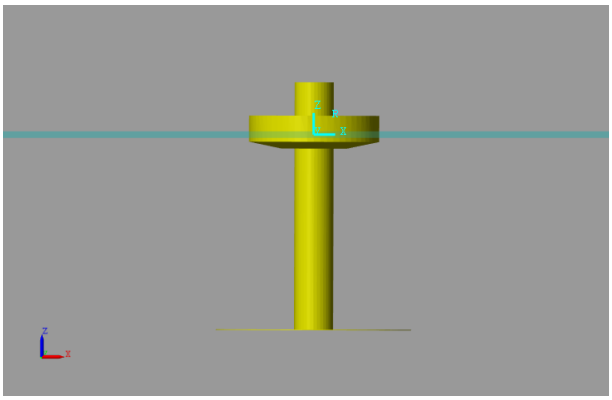

Fig. 8. The RM3 point absorber with still water level and coordinate system.

The run time of each sea state was 3600s with 100s ramp time and a time step of 0.1s. Taking an illustrative example from method C, the representative sea state from the 15th sub-plot containing 183 spectra in Fig. 6, is shown in Fig. 9. The wave elevation signal is obtained from the following equation (8) and (9) [21]:

$$\zeta = \sum_{j=1}^{N} A_j \sin(\omega_j t - k_j x + \epsilon_j) \quad (8)$$

in which A_j, ω_j, k_j, ϵ_j are the wave amplitude, angular frequency, wave number and random phase angle for frequency component f_j. The relationship with wave amplitude and wave spectrum is shown below:

$$\frac{1}{2} {A_j}^2 = S(\omega_j) \Delta\omega \quad (9)$$

in which $S(\omega)$ is the wave spectrum. The wave elevation time signal for the example from equation (8) is shown in Fig. 10.

Using this wave signal as the input to the WEC-SIM model, the relative movement between two bodies is obtained, and the power output time history calculated using equation (8), which is shown in Fig. 11. The average power output is calculated by equation (10).

$$P_{average} = \frac{1}{T_2 - T_1} \int_{T_1}^{T_2} p(t) dt \quad (10)$$

in which p is the instantaneous power output, T_1 and T_2 are the lower and upper boundaries of the time window selected for the power output calculation, taken once initial transients have settled, between T_1 =200s and T_2 =3600s. For this representative sea state, the average power output is 1.12E05W [22].

Each of the representative sea states is calculated accordingly, the results from method C is shown in Table

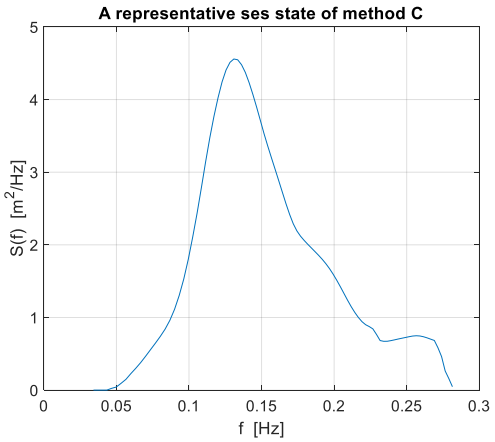

Fig. 9. A representative sea state of method C

IV as an example, the value of k corresponds to the order of subplots in Fig. 6. Then each method's group members' average power output (3161 sea states) is obtained using the same method. Then comparing the representative power output with each group member's average power output with the metric in equation (6) to check the regrouping quality, the result is shown in Fig. 12.

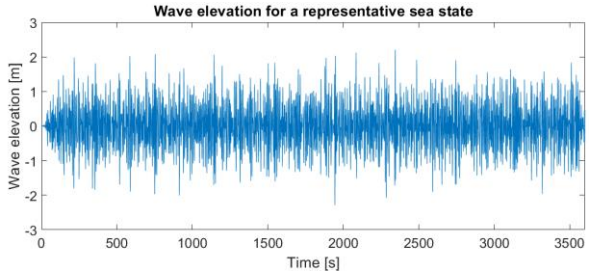

Fig. 10. Wave elevation signal of a representative sea state of method C.

It can be seen that the result is very similar to Fig. 4 for the parameter *Power*, In Fig. 4, the *Power* represents the wave power, while in Fig. 12, the metric is for average power output by using those representative sea states from the model. It can be seen for a linear WEC model, the power output presents a linear relationship with the wave power input. The representative wave power from different regrouping methods are directly reflected on the average power output. From Fig. 12, the representative sea states from method C presents the lowest metric value of average power output, according to the definition of metric from equation (6), the lower the value is, the higher

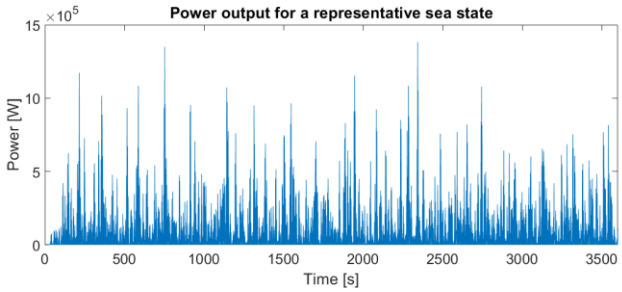

Fig. 11. Power output of a representative sea state of method C

representativeness it has. Which means the average power output obtained from the representative sea states from method C has the lowest average difference from its group members.

From the results shown in Fig. 12, method A and B are binning methods, they provide a relative lower

TABLE IV
POWER OUTPUT OF METHOD C

k	1	2	3	4	5
N_k	8	16	7	20	30
P_k [W]	5.02E+05	3.66E+05	4.28E+05	2.63E+05	3.40E+05
E_k [kW.h]	4.01E+03	5.85E+03	3.00E+03	5.26E+03	1.02E+04
k	6	7	8	9	10
N_k	40	40	64	85	95
P_k [W]	2.58E+05	1.64E+05	2.36E+05	1.62E+05	1.78E+05
E_k [kW.h]	1.03E+04	6.56E+03	1.51E+04	1.38E+04	1.69E+04
k	11	12	13	14	15
N_k	86	114	63	215	183
P_k [W]	1.03E+05	1.49E+05	5.34E+04	8.98E+04	1.12E+05
E_k [kW.h]	8.88E+03	1.70E+04	3.36E+03	1.93E+04	2.04E+04
k	16	17	18	19	20
N_k	203	298	327	527	740
P_k [W]	7.75E+04	6.64E+04	4.54E+04	4.12E+04	1.82E+04
E_k [kW.h]	1.57E+04	1.98E+04	1.48E+04	2.17E+04	1.35E+04

representativeness as expected because they regroup sea states by only considering H_s and T_e by a number of equally sized bins and sea states with very different wave energy can be grouped together. Method C (non-directional wave spectrum K-means clustering method) has the highest representativeness regarding to power output. Method D (directional wave spectrum clustering) performs a relative low representativeness for wave power regrouping and the average power output regrouping as

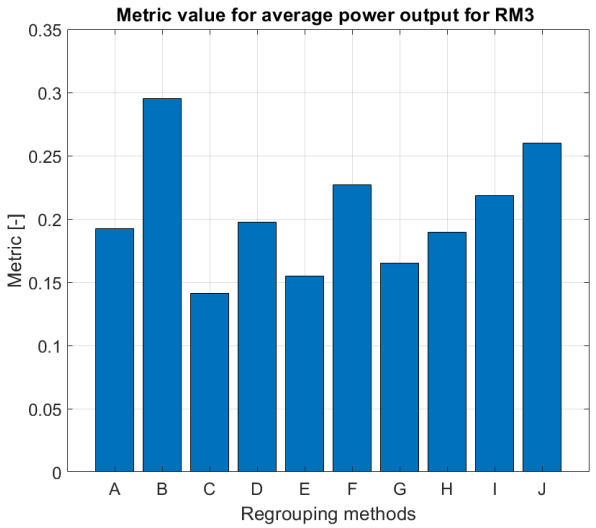

Fig. 12. Metric for average power output of RM3 point absorber.

well. It is because during the regrouping process for sea states, the influence of wave spreading direction θ is taken into consideration, however, during the calculation for wave power (not power output from the model), the directionality has no direct relationship to the wave power for this RM3 model. According to previous analysis [2], taking into account one parameter in the K-means clustering process will always reduce the influence of other parameters which explains why the representativeness from method D is not as high as method C. Similarly, for average power output analysis, since the power output of a point absorber is not affected by the directionality of the waves either, the consideration of wave direction θ cannot be reflected in the power output, that is why method D also shows a lower representativeness relative to method C.

What is worth mentioning is method I and J, they are both two-step methods [2] in order to find a balance between obtaining a high representativeness and a high uniformity in *Hs-Te* space, but they both show a lower representativeness using the metric in this paper.

From the result of the analysis, sea states obtained from method C provides the highest representativeness for the average power output for the RM3 WEC and also a second highest representativeness for the wave power. The difference between Fig. 4 and Fig. 12 is due to the random phase angle generated for power output calculation. As a result, the representative sea states from method C are recommended for model testing of the RM3 WEC

G. *Total energy output estimation by WEC-SIM*

The accurate total energy extracted by the RM3 point absorber from the original 3161 sea states was calculated from the average power result for each sea state and assuming each state lasted 1 hour. Each of the sea state uses a random phase angle ranging from 0 to 2π. This resulted in a total energy extraction of 2.456e+05kW.h. This value is considered as the accurate total energy output.

This value is compared with the total power estimated using the representative sea states, which is calculated by the following equations (11) to (12):

$$E_k = P_k * N_k * 3600 \tag{11}$$

Then

$$E_{total} = \sum_{k=1}^{K} E_k \tag{12}$$

In which k is group label k (1,2,3…K), N_k is the number of members in group k, P_k is the average power output of the representative sea state of group k. E_k is the total energy output for 1 hour of each representative sea state in group k. E_{total} is the energy output for all of the K groups together which is also 3161 hours. The unit of the energy obtained from equation (12) is in J, this value is then transformed to kW.h.

It is found that each method's total energy output prediction is very similar, with small differences. In order to find out if these differences were due to the influence of the random phase angles used to generate wave time series from the representative wave spectra, the total power calculation from the 10 methods were repeated twice, and each time the phase angle is different. In total there are 3 sets of total energy output estimation results, see Table V and Fig.13, which summarise the energy predictions for each method and the relative error in % compared with the total energy output summed using all sea states.

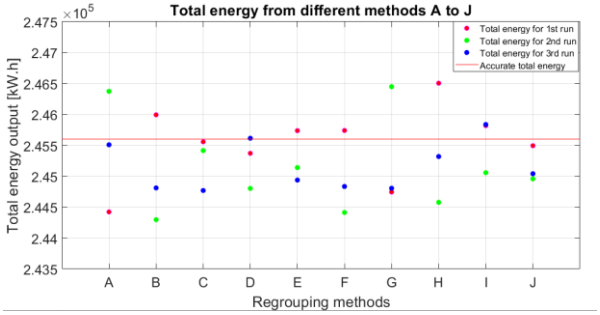

Fig. 13. Total energy estimation from methods A to J.

From the results it can be seen that each method predicts the total energy output with the relative error ranging from -0.5% to +0.5%. This error is due to the random phase angle generated each run.

H. *Total Energy estimation with parametric JONSWAP wave spectrum*

The total energy estimated from the 1st run shown in Table V is compared in Fig. 14 with the total energy estimated using the H_{m0} and T_p from these sea states applied to the JONSWAP spectrum. The equation for a JONSWAP wave spectrum is shown in the following equations (13) to (19) [22].

$$S(f) = [1 - 0.287ln(\gamma)]S_{PM}\gamma^{\alpha} \tag{13}$$

in which S_{PM} is Pierson–Moskowitz (PM) spectrum with γ=3.3, and:

$$S_{PM} = \frac{{H_{m0}}^2}{4}(1.057f_p)^4 f^{-5}\exp[-\frac{5}{4}\left(\frac{f_p}{f}\right)^4] \tag{14}$$

in which

$$H_{m0} = 4\sqrt{m_0} \tag{15}$$

and

$$m_0 = \int_0^{\infty} S(f)df \tag{16}$$

Then

$$\alpha = exp[-(\frac{\frac{f}{f_p}-1}{\sqrt{2}\sigma})^2] \tag{17}$$

in which

$$\sigma = \begin{cases} 0.07 & f < f_p \\ 0.09 & f > f_p \end{cases} \quad (18)$$

H_{m0} is the significant wave height, and f_p is the peak frequency of the spectrum.

$$f_p = \frac{1}{T_p} \quad (19)$$

Each regrouping method's representative sea state can then be transformed into JONSWAP wave spectrum. Each spectrum was imported to WEC-SIM, the run time is also 3600s with 100s ramp time. The average power output for each sea state from 200 s to 3600s are obtained. Then the total energy output for 3161 hours estimated by using the JONSWAP spectrum can be obtained, which is shown in Table VI.

TABLE V
TOTAL ENERGY ESTIMATION RELATIVE ERROR METHOD A TO J [%]

METHOD	A	B	C	D	E
1ST RUN	-0.48	0.16	-0.02	-0.09	0.06
2ND RUN	0.31	-0.53	-0.08	-0.32	-0.19
3RD RUN	-0.04	-0.32	-0.34	0.01	-0.27
MEAN VALUE	-0.07	-0.23	-0.15	-0.13	-0.13
STANDARD DEVIATION	0.32	0.29	0.14	0.14	0.14
METHOD	F	G	H	I	J
1ST RUN	0.06	-0.35	0.37	0.09	-0.04
2ND RUN	-0.48	0.35	-0.42	-0.22	-0.26
3RD RUN	-0.31	-0.32	-0.11	0.10	-0.23
MEAN VALUE	-0.24	-0.11	-0.05	-0.01	-0.18
STANDARD DEVIATION	0.23	0.32	0.32	0.15	0.10

The results is plotted in Fig. 14, with the results from complex sea states from Table V for comparison, it can be seen that compared with the total energy output by using the complex sea states 1st run from HF radar data, the results from the JONSWAP spectrum is significantly different. The total energy is always over-predicted and the average relative error from using the JONSWAP spectrum is between 2.9% (method G) to 7.7% (method B), which is much larger than the total energy predicted by using representative sea states (±0.5%).

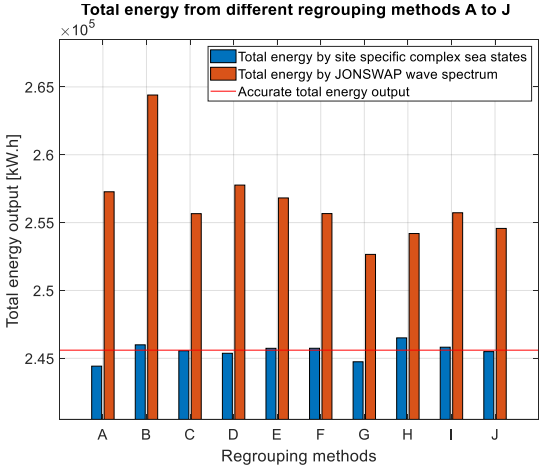

Fig. 14. Total energy estimation by different regrouping methods.

What's worth mentioning is that although all of the 10 regrouping methods obtains an accurate total energy output for this linear RM3 model, it is not the case for traditional binning method from Fig.2. It is because the 15 bins shown in Fig.2 cannot represent all of the sea states from the figure as most of the sea states are left outside the selected bins. Even if we obtain the average power output from 15 selected bins from tank testing, it is impossible to use these results to have an accurate total energy estimation due to the fact that the average power output from the unselected bins are unknown.

As a result, method C does show an obvious advantage on selecting the sea states for tank testing and estimating the total energy output for this linear RM3 WEC.

IV. CONCLUSIONS

10 regrouping methods to obtain the representative sea states have been used on HF radar measured wave spectrum data. The results have been tested for a RM3 point absorber numerical model using WEC-SIM, a MATLAB based open-sourced software. The average power output from the representative sea states of each method have been evaluated by a metric. It is shown that the non-directional wave spectrum K-means clustering method (method C) provides the most representative power output, which means these representative sea states from method C are recommended for selection in model tests.

The representative sea states from different methods were used to make an estimation for the total energy output prediction in a given time period (3161 hours), it is shown that by using the complex sea states (non-directional spectrum), all of the 10 methods provide similar estimates of the energy within ±0.5% accuracy, which is impossible by using the traditional binning methods. The performance of the regrouping methods in representing the sea state, power conversion and total energy output show a similar distribution. This is due to the high linearity of the RM3 model and its response in the sea states tested. For the case tested here, the total energy output is shown to be predicted with an accuracy of within ±0.5% no matter which regrouping method we use. A highly non-linear WEC model and different sea states will be tested in the future work.

The same representative sea states from different methods were transformed into H_s-T_p JONSWAP wave spectra for total energy estimation for comparison and found consistently to over-predict the total power capture with a significant error, much larger than for the complex sea states.

RM3 WEC is a point absorber, which is not sensitive to the wave direction. In the further, other types of devices that are wave direction sensitive needs to be tested in the representative sea states to find out the most suitable method for sea states selection.

ACKNOWLEDGEMENT

The research leading to these results has received funding from the European Union Horizon 2020 Framework Programme (H2020) under grant agreement no 731084.

REFERENCES

[1] S. Draycott, "On the Re-creation of Site-Specific Directional Wave Conditions," 2017.

[2] D. Wang, D. Conley, M. Hann, K. M. Collins, and D. Greaves, "Use of HF radar for replciating wave-current combined wave conditions for testing of wave energy converters," 2019.

[3] K. Koca, A. Kortenhaus, and H. Oumeraci, *Recent Advances in the Development of Wave Energy Converters*. 2013.

[4] F. Mahnamfar and A. Altunkaynak, "Comparison of numerical and experimental analyses for optimizing the geometry of OWC systems," *Ocean Engineering,* vol. 130, pp. 10-24, 2017/01/15/ 2017.

[5] G. Mørk, S. Barstow, A. Kabuth, and M. T. Pontes, "Assessing the Global Wave Energy Potential," 2010. Available: https://doi.org/10.1115/OMAE2010-20473

[6] M. Héder, "From NASA to EU: the evolution of the TRL scale in Public Sector Innovation."

[7] D. M. Ingram, *Protocols for the equitable assessment of marine energy converters*. 2011.

[8] K. Hasselmann *et al.*, "Measurements of wind-wave growth and swell decay during the Joint North Sea Wave Project (JONSWAP)," *Ergänzungsheft 8-12,* 1973.

[9] L. J. Hamilton, "Characterising spectral sea wave conditions with statistical clustering of actual spectra," *Applied Ocean Research,* vol. 32, no. 3, pp. 332-342, 2010/07/01/ 2010.

[10] J. Han and M. Kamber, "Data Mining: Concepts and Techniques, chapter Mining association rules in large databases," ed: Morgan Kaufmann Publisher, 2001.

[11] S. F. Barstow, J.-R. Bidlot, and S. Caires, "Measuring and analysing the directional spectrum of ocean waves," ed: COST Office, 2005.

[12] D. D. Crombie, "Doppler spectrum of sea echo at 13.56 Mc./s," *Nature,* vol. 175, no. 4459, p. 681, 1955.

[13] L. R. Wyatt, "Limits to the Inversion of HF Radar Backscatter for Ocean Wave Measurement," *Journal of Atmospheric and Oceanic Technology,* vol. 17, no. 12, pp. 1651-1666, 2000.

[14] J. J. Green and L. R. Wyatt, "Row-Action Inversion of the Barrick–Weber Equations," *Journal of Atmospheric and Oceanic Technology,* vol. 23, no. 3, pp. 501-510, 2006.

[15] R. Carballo and G. Iglesias, "A methodology to determine the power performance of wave energy converters at a particular coastal location," *Energy Conversion and Management,* vol. 61, pp. 8-18, 2012/09/01/ 2012.

[16] S. B. J Ohana, V Baudry, F. Thiebaut, and M. H. Keri Collins, Carlos Perez Collazo,Tom Davey, "D4.1-2 Common MaRINET 2 standard testing and benchmarking plan_WAVES_v4," 2019.

[17] S. Draycott, T. Davey, D. Ingram, J. Lawrence, A. Day, and L. Johanning, "Applying site specific resource assessment: Methodologies for replicating real seas in the FLOWAVE facility," presented at the International Conference on Ocean Energy (ICOE), 2014-11-06, 2014.

[18] Y. Yu, M. Lawson, Y. Li, M. Previsic, J. Epler, and J. Lou, "Experimental wave tank test for reference model 3 floating-point absorber wave energy converter project," National Renewable Energy Lab.(NREL), Golden, CO (United States)2015.

[19] M. Lawson, Y.-H. Yu, K. Ruehl, and C. Michelen, "Development and demonstration of the WEC-Sim wave energy converter simulation tool," 2014.

[20] Website for RM3 point absorber dimensional parameters. Available: https://wec-sim.github.io/WEC-Sim/man/tutorials.html

[21] O. Faltinsen, *Sea loads on ships and offshore structures*. Cambridge university press, 1993.

[22] Official website of WEC-SIM. Available: https://wec-sim.github.io/WEC-Sim/master/theory/theory.html#irregular-waves